18th Brazilian Congress of Thermal Sciences and Engineering
November 16-20, 2020 (Online)

ENC-2020-0259
DIRECT EXPANSION HEAT PUMP EVAPORATOR MATHEMATICAL MODELING FOR THE SELECTION OF A REFRIGERANT WITH OPTIMIZED ENVIRONMENTAL PERFORMANCE

Hélio Augusto Goulart Diniz
Federal University of Minas Gerais (UFMG), Post-Graduate Program in Mechanical Engineering, Av. Antonio Carlos, 6627 – Pampulha, Belo Horizonte - MG, 31270-901, Brazil
Federal University of Minas Gerais (UFMG), Department of Mechanical Engineering, Av. Antonio Carlos, 6627 – Pampulha, Belo Horizonte - MG, 31270-901, Brazil
University Center Estácio de Sá, Av. Francisco Sales, 23 – Floresta, Belo Horizonte - MG, 30150-220, Brazil
Faculty of Education of Minas Gerais (FACEMG)/ Belo Horizonte Institute of Higher Education (IBHES), Av. Vilarinho, 2395 – Venda Nova, Belo Horizonte - MG, 31615-250, Brazil
heliomecanica@ufmg.br

André Gonçalves de Oliveira
Stella Marys Silva Pinheiro
Federal University of Minas Gerais (UFMG), Department of Mechanical Engineering, Av. Antonio Carlos, 6627 – Pampulha, Belo Horizonte - MG, 31270-901, Brazil
andreqix@hotmail.com, stella_marys_@hotmail.com

Luiz Machado
Raphael Nunes de Oliveira
Federal University of Minas Gerais (UFMG), Post-Graduate Program in Mechanical Engineering, Av. Antonio Carlos, 6627 – Pampulha, Belo Horizonte - MG, 31270-901, Brazil
Federal University of Minas Gerais (UFMG), Department of Mechanical Engineering, Av. Antonio Carlos, 6627 – Pampulha, Belo Horizonte - MG, 31270-901, Brazil
luizm@demec.ufmg.br, rphnunes@demec.ufmg.br

Abstract. *The mathematical modeling of heat exchangers is explored by the scientific community in studies of thermal equipment to evaluate the feasibility of replacing traditional refrigeration fluids with ecological fluids and their impact on the system energy efficiency. The present work aims to present the evaporator mathematical modeling of a Direct-Expansion Solar Assisted Heat Pump (DX-SAHP) used to residential water heating combined with the selection procedure for a friendly refrigerant. The methodology is based on dimensioning the heat exchanger and evaluating, through computer simulations, the global energy efficiency of the system and the Total Equivalent Warming Impact (TEWI) using the following refrigerants that have low GWP (Global Warming Potential) and ODP (Ozone Depleting Potential) zero: R152a, R744, R1234yf, R1234ze (E), R1233zd (E), R170, R290, R600 and R600a. The goal of this work is to develop a useful tool for selecting an appropriate ecological refrigerant to be used in a solar heat pump depending on the required operating conditions. The main result is the selection of R290 to operate the proposed system. This study has allowed the development of a useful tool for the selection of the appropriate ecological refrigerant of a low cost residential solar heat pump.*

Keywords: *Mathematical modeling, DX-SAHP, evaporator, TEWI, ecological fluids.*

1. INTRODUCTION

The use of solar heat pumps for water heating has stood out due to the significant energy savings compared to electrical resistance and gas heaters. Within this context, a solar heat pump, with the purpose of heating water for residential use, was designed and built by the Refrigeration and Heating Group (GREA) of the Federal University of Minas Gerais (UFMG), resulting in master's and PhD thesis (Reis, 2012; Rodríguez, 2015; Diniz, 2017).

The replacement of traditional synthetic fluids, HFCs (hydrofluorocarbons), with fluids with low environmental impact, zero ODP and low GWP, has started to be explored more intensely in recent decades by the industry and academic community looking for better energy efficiency and environmental efficiency in cooling and heating systems and equipment. This issue was further intensified in 2016 by the Kigali Amendment (UNEP, 2016) of the Montreal protocol

that defined a strict timetable for reducing the production and consumption of HFCs (Ruas, 2018). Among the current refrigeration fluids with low environmental impact, the following stand out: natural fluids, especially carbon dioxide (CO2) due to the absence of toxicity in relation to other natural fluids. The CO2 has the lowest GWP of all refrigerants, being the reference for this index. Moreover, it was one of the first refrigerant fluids applied in refrigeration. It was forgotten for decades by the advent of synthetic fluids, however, has returned to be applied on a large scale due to the restrictions of the Montreal protocols and Kyoto (Faria, 2013; Oliveira, 2013). HCs (hydrocarbons), which have a similar historical context to natural fluids and which are currently being widely applied by the industry and explored by researchers, especially R600a (isobutane) and R290 (propane). And finally, the Hydrofluoroolefins (HFOs), belonging to the fourth generation of fluorinated fluids, especially the R1234yf, developed for the retrofit of the R134a in the air conditioning system of new cars produced in Europe (Bobbo et al., 2014).

Some works in this research segment have already been carried out, evaluating the energy and environmental performance of heat pumps for heating with replacement of traditional fluids by fluids with low environmental impact, according to Table 1.

Table 1. Works on fluid replacement in heat pumps.

Authors	Thermal Systems	Fluids evaluated
Park e Jung (2009)	Heat pump	R170/R290/ R22
Barve e Cremaschi (2012)	Residential heat pump	R32/R1234yf/R410A
Zhang e Muehlbauer (2012)	Residential heat pump	R410A/R134a/R1234yf
Makhnatch e Khodabandeh (2014a); Makhnatch e Khodabandeh (2014b)	Air-water heat pump	R410A/R290/R1270/ R152a/R1234yf
Ju et al. (2017)	Heat pump for water heating	R1233zd(E)/ R22/R134a/ R1270/R290
Nawaz et al. (2017a)	Heat pump for water heating	R1234yf/R1234ze(E)/ R134a
Nawaz et al. (2017b)	Heat pump for water heating	R290/R600a/ R134a
Koyama et al (2018)	Water-to-water heat pump	R32/R1123
Ju et al. (2018a); Ju et al. (2018b)	Water-to-water heat pump	R744/R290/R22
Duarte et al. (2019)	DX-SAHP for water heating	R290/R600a/R744/R1234yf/ R134a
Xiao et al. (2020)	DX-SAHP for water heating	R290/R600a/R13I1/R134a
Bai et al. (2020)	DX-SAHP for water heating	R32/R290/R600a/ R134a

The purpose of this article is to present the evaporator mathematical modeling of a DX-SAHP for residential use and describe the procedure for selecting a friendly refrigerant. This work simulates and critically evaluates energy efficiency, through the performance coefficient (COP) and TEWI, of the following selected fluids: R152a, R744, R1234yf, R1234ze(E), R1233zd(E), R170, R290, R600 e R600a.

2. METHODOLOGY

The mathematical modeling of the heat exchangers will enable the construction of the system. The proposed heat pump prototype is a steam compression heating system, with the primary working fluid being a low GWP and TEWI refrigerant, and as secondary fluids, air in the evaporator and water in the condenser. The machine is basically composed of a hermetic compressor with fixed rotation, a coil-shaped flooded condenser, a countercurrent coaxial condenser, a flat plate solar evaporator and three capillary tubes. In addition, it has a thermal reservoir with a storage capacity of 200 L where the condenser is installed at the bottom by immersion.

Heat exchangers are sized (in this case only the evaporator is sized) and the necessary mass of refrigerant for the correct functioning of the system is calculated for the different refrigerants. The EES software (Klein and Alranrado, 2015) was used for the heating pump project and for all fluids and solids properties calculation.

2.1 Environmental performance indicators

Different environmental indicators are used to facilitate the decision-making process for selecting a refrigerant with low global warming potential. The three conventional and most applied environmental indicators in the literature are: GWP, TEWI and life cycle climate performance (LCCP) (Makhnatch and Khodabandeh, 2014b).

GWP is the most widely used environmental indicator. This index compares the global warming impact of a greenhouse gas emission with the impact of emitting a similar amount of CO_2. The impact is estimated over a time horizon. A 100-year time horizon is the most commonly assumed when no information about the time horizon is provided. GWP is an indicator easy to use, the lower the GWP, the less a substance contributes to global warming. GWP is a useful

indicator for comparing different refrigerants. However, it can overestimate the benefits of low GWP refrigerant to the environment, as it does not take into account many other factors that affect it (Makhnatch and Khodabandeh, 2014b).

In addition to the direct influence of the refrigerant (which is conveniently estimated by the GWP), any system or process that requires energy input indirectly affects the environment. This impact is due to the CO_2 emissions from energy production processes. To indicate the overall environmental impact of a cooling or heating system during its operation, another environmental indicator, called TEWI, is used. The TEWI indicates the global warming impact of direct and indirect emissions and it is calculated as a sum of both: the direct effect of the refrigerant released during the life of the equipment and the indirect impact of CO_2 emissions from fossil fuels used to generate energy to operate the equipment throughout its life depending on the type of energy matrix in the country. The TEWI is simpler to be used as environmental indicator than LCCP and more correct than GWP when selecting a low GWP refrigerant that is environmentally friendly. The TEWI is influenced by the system energy performance. Thus, the efficiency of the cooling or heating system may be the most important parameter in estimating the system environmental impact (Zhang and Muehlbauer, 2012; Makhnatch and Khodabandeh, 2014b). The TEWI (kg-CO2) can be calculated using Eq. (1) to Eq. (5) (Antunes and Bandarra Filho, 2016; Paula and Duarte, 2019).

$$TEWI = TEWI_{Direct} + TEWI_{Indirect} \quad (1)$$

$$TEWI_{Direct} = m_f . L_{rate} . L_{time} . GWP + m_f . (1 - \alpha_{TEWI}) . GWP \quad (2)$$

$$TEWI_{Indirect} = E_{Annual} . \beta_{TEWI} . L_{time} \quad (3)$$

$$E_{Annual} = 365 . t_{oper} . \frac{\dot{Q}_{evap}}{COP} \quad (4)$$

$$E_{Annual} = 365 . t_{oper} . \frac{\dot{Q}_{cond}}{COP} \quad (5)$$

On what $m_f$is the system refrigerant mass (kg), $L_{rate}$is the annual rate of refrigerant emitted (by replacement and leakage of the system) (%/year), L_{time} is the life of the system (year), α_{TEWI} is the recovery rate of refrigerant life (%), E_{Annual} is the system electricity annual consumption (kWh/year), β_{TEWI} is the carbon dioxide emission factor per kWh of energy produced by the country's energy matrix (kg-CO2/kWh) and t_{oper} is the equipment daily operation time (h/day). Eq. (4) is applicable to a cooling machine with cooling capacity $\dot{Q}_{evap}$ (kW) and Eq. (5) is applicable to a heat pump with heating capacity $\dot{Q}_{cond}$ (kW). To determine the TEWI of a heat pump operating in Brazil, the values shown in Table 2 were assumed.

Table 2. Values and references for TEWI parameters.

Parameter	Considerations	Reference
$L_{rate} = 12{,}5\%$	Centralized system, normal operation, catastrophic losses during service and maintenance.	AIRAH (2012); Antunes e Bandarra Filho (2016); Paula e Duarte (2019).
$L_{time} = 15\ years$	Equipment that operates with economical useful life.	Makhnatch e Khodabandeh (2014a); Makhnatch e Khodabandeh (2014b); Paula e Duarte (2019).
$\alpha_{TEWI} = 70\%$	Refrigerant mass less than 100 kg.	AIRAH (2012); Antunes e Bandarra Filho (2016); Paula e Duarte (2019).
$\beta_{TEWI} = 0{,}082$ kgCO2 /kWh	Reference value for Brazil.	Antunes and Bandarra Filho (2016).
$t_{oper} =$ 12 hours	Estimated value in daily use.	Paula e Duarte (2019).
$\eta_{comp} =$ 0,50 (overall compressor efficiency)	Value assumed for all refrigerants.	Diniz (2017); Paula e Duarte (2019).

Computer simulations are performed using the EES software (2015) for the ecological refrigerants indicated in Table 1 and refrigerants with GWP below 150, a procedure analogous to the methodology assumed by Makhnatch and

Khodabandeh (2014a) and Makhnatch and Khodabandeh (2014b). It should be noted that only refrigerants with ODP equal to zero and available in the thermophysical properties software library were analyzed. The GWP values were consulted in ASHRAE (2017). The following refrigerants were evaluated: R152a, R744, R1234yf, R1234ze (E), R1233zd (E), R170, R290, R600 and R600a. R134a is also analyzed for comparative reasons with the works of Reis (2012), Rodríguez (2015) and Diniz (2017).

2.2 Modeling the solar evaporator

There are two types of situations in which a DX-SAHP can be used. The first refers for the system operating indoor, inside the laboratory, out of the influence of wind and solar radiation. The second situation refers to when the system operates outdoors, in an open environment exposed to solar radiation and the action of the wind. For sizing the evaporator, a scenario with medium environmental conditions to indoor and outdoor conditions was considered. The average values of the parameters involved in the problem are based on the extensive test bench available in the work of Diniz (2017), which performed tests in both conditions with a DX-SAHP (operating with R134a) similar to the one dimensioned in this work. The exception is the temperature of the sky, which is based on the work of Duarte (2018). The procedures for sizing are based on the works of Faria (2013) and Diniz (2017).

The evaporator chosen to compose DX-SAHP is the flat plate type evaporator shaped on the surroundings of a coil-shaped tube, also known as solar evaporator. This evaporator has been providing higher energy efficiency to heat pumps than other types of evaporators, especially when exposed to solar irradiation. The solar evaporator can receive heat by five means: by natural convection imposed by the ambient air, by forced convection of the air imposed by the wind, by the latent heat of water vapor condensation present in the air, by the solar irradiation and by the ambient radiation. This achieves a considerable increase in the heat exchange coefficient of the refrigerant. Finally, it is worth mentioning that the DX-SAHP dimensioned in this article has a heating capacity of 900 W. This condition is the starting point for the design of the entire system.

The solar evaporator acts as a collector, being modeled as a long fin and isolated at the ends (adiabatic sides). The tube has the function of the base of the fin, with the refrigerant flowing at low temperature inside. The fin flaps, fixed symmetrically to the tube, act as extended surfaces that captured heat from the environment to the tube, which is absorbed by the refrigerant. However, since the fin flaps are usually short, the resulting length of the component is relatively long. With this, the fin is arranged in parallel sections to make it compact. The end result is a plate formed into a serpentine-shaped tube. Figure 1 shows the cross section of the plate.

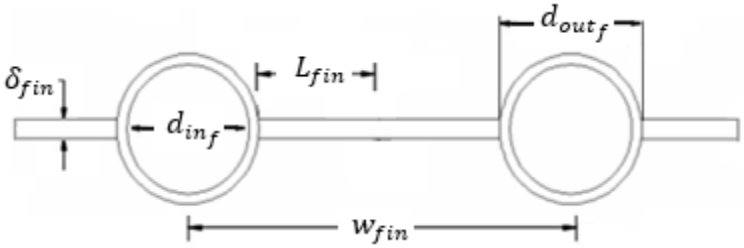

Figure 1: Fin cross section.

The designed solar evaporator can be analyzed, from a constructive point of view, as being composed of an aluminum plate and a copper tube arranged in the shape of a serpentine. The set is close to that of a gray body, whose absorptivity and emissivity are worth 0.95. Table 3 presents the parameters defined for the project.

Table 3: Parameters for dimensioning the solar evaporator.

Parameters and Characteristics	Materials and values
Initial temperature of refrigerating fluid	T_{f_2} = 74 °C
Final temperature of refrigerating fluid	T_{f_3} = 45 °C
Condensing temperature of refrigerating fluid	$T_{f_{cd}}$ = 52 °C
Tube material	Cupper
Board material	Aluminum
Inner tube diameter	d_{in_f} = 7.94 mm
Tube outside diameter (3/8 inch)	d_{out_f} = 9.53 mm
Tube wall thickness	0.795 mm
Fin thickness	δ_{fin} = 1 mm
Distance between tubes center to center	w_{fin} = 103 mm
Characteristic fin length	L_{fin} = 46.74 mm

Parameters and Characteristics	Materials and values
Initial temperature of refrigerating fluid	T_{f_2} = 74 °C
Final temperature of refrigerating fluid	T_{f_3} = 45 °C
Condensing temperature of refrigerating fluid	$T_{f_{cd}}$ = 52 °C
Characteristic plate length	L_{pl} = 1.60 m
Inclination of the evaporator with the vertical	θ = 60º
Plate emissivity	ε = 0.95
Plate absorptivity	λ = 0.95
Solar irradiation flow	I_{solar} = 500 W/m²
Ambient temperature	T_{amb} = 25 ºC
Surrounding temperature	T_{sur} = 25 ºC
Air temperature	T_{air} = 25 ºC
Sky temperature	T_{sky} = 0 ºC
Atmospheric pressure	P_{atm} = 102.2 kPa
Relative humidity	ϕ = 50%
Average air speed	V_{air} = 0.52 m/s
Inlet refrigerant temperature	T_{f_4} = 5 ºC
Boiling temperature (saturation temperature)	T_{f_b} = 5 ºC
Outlet refrigerant temperature	T_{f_1} = 12 ºC
Overheating	T_{OH} = 7 ºC

The fin surface is responsible for most of the heat transfer from the evaporator. However, not all of the physically available area is used for this purpose, and it is essential to determine the efficiency η_{fin} of the fin surface use for thermal exchanges using Eq. (6), in which M is the fin coefficient, given by Eq. (7).

$$\eta_{fin} = \frac{\tanh(ML_{fin})}{ML_{fin}} \tag{6}$$

$$M = \sqrt{\frac{H_{amb}Pe_{fin}}{A_{cs}k_{fin}}} \tag{7}$$

Where Pe_{fin} is the perimeter of the area exposed to heat flow through the fin given by Eq. (8), A_{cs} is the area of the cross section to the heat flow through the fin given by Eq. (9), k_{fin} is the thermal conductivity of the material that constitutes the fin and H_{amb} is the heat transfer coefficient of the environment, being modeled mathematically later.

$$Pe_{fin} = 2L_{evap} + 2\delta_{fin} \tag{8}$$

$$A_{cs} = L_{evap}\delta_{fin} \tag{9}$$

On what L_{evap} is the length of the evaporator tube. The following parameters are important for determining the heat rates exchanged between the evaporator and the environment (shown below): the area of one face of the fin A_{fin} given by Eq. (10) and the area of the base of the fin A_b given by Eq. (11).

$$A_{fin} = 2L_{evap}L_{fin} \tag{10}$$

$$A_b = \pi d_{out_f}L_{evap} - 2\delta_{fin}L_{evap} \tag{11}$$

The mass flow of the refrigerant $\dot{m}_f$ is calculated by Eq. (12) and depends on enthalpies at the condenser inlet h_{f_2} and outlet h_{f_3}. The Index "2" is used for the condenser inlet (compressor outlet) and the index "3" for the condenser outlet (expansion device inlet). It is assumed that the condensation process occurs at constant pressure.

$$\dot{Q}_{cond} = \dot{m}_f(h_{f_2} - h_{f_3}) \tag{12}$$

For the CO_2 gas cooler, T_{f_2} = 65 ºC and T_{f_3} = 30 ºC are assumed. In addition to these data, it is necessary to define the highest pressure, at which the cooling process occurs, it is considered P_{high} = 7600 kPa. The same procedure is assumed for R170, however, it is considered P_{high} = 5000 kPa.

The heat transfer in an evaporator occurs in two different regimes, corresponding to the refrigerant boiling and overheating steps. For each of these regions it is necessary to calculate the corresponding length in which the respective process takes place. The thermal load of the boiling region $\dot{Q}_b$ is given by Eq. (13) and the thermal load of the overheating region $\dot{Q}_{OH}$ is given by Eq. (14). Finally, Eq. (15) presents the total thermal load related to the heat exchanger, also known as cooling capacity $\dot{Q}_{evap}$.

$$\dot{Q}_e = \dot{m}_f(h_{f_4} - h_{f_1,}) \tag{13}$$

$$\dot{Q}_{OH} = \dot{m}_f(h_{f_1,} - h_{f_1}) \tag{14}$$

$$\dot{Q}_{evap} = \dot{Q}_e + \dot{Q}_{OH} \tag{15}$$

The thermal capacity of the evaporator depends on the enthalpy at its inlet h_{f_4} and outlet h_{f_1}. The process that occurs in the expansion device is considered to be isentalpical, therefore h_{f_4} has the same value as h_{f_2}. It is used the Index "4" for the evaporator inlet (outlet of the expansion device) and the Index "1" for the evaporator outlet (compressor inlet). Thus, heat from the environment is absorbed by the refrigerant, causing it to evaporate and overheat. Finally, $h_{f_1,}$ is the enthalpy of the refrigerant on the border between the boiling region and the superheating region.

The first region to be dimensioned is the boiling region of the refrigerating fluid. This stage is characterized by the phase change of the fluid in the biphasic state liquid-vapor to saturated vapor, absorbing a large amount of energy from the environment, due to the high coefficient of heat transfer by boiling. At this stage, the temperature of the refrigerant does not vary, being at points 4 and 1' equal to T_{f_b}. To determine the length of the boiling region L_b, Eq. (16) is used.

$$\dot{Q}_b = U_b \pi d_{out_f} L_b (T_{amb} - T_b) \tag{16}$$

On what U_b is the global coefficient of the refrigerant in the boiling region given by Eq. (17) and the wall temperature in the region T_{w_b} is given by Eq. (18). Where k_w is the thermal conductivity of the tube at wall temperature in the region.

$$\frac{1}{U_b} = \frac{1}{H_{amb}} + \frac{d_{out_f}}{H_{f_b} d_{in_f}} + \frac{d_{out_f} In\left(\frac{d_{out_f}}{d_{in_f}}\right)}{2k_w} \tag{17}$$

$$T_{w_b} = \frac{H_{f_b} T_{f_b} + H_{amb} T_{amb}}{H_{f_b} + H_{amb}} \tag{18}$$

Where H_{f_b} is the internal heat transfer coefficient of the refrigerant in the boiling region. According to Koury (1998), for the calculation of H_{f_b}, one must take into account that the boiling process is divided into two parts. The first part is called the full boiling zone, where it starts with the refrigerant fluid in the low vapor quality state x_{in} at the evaporator inlet and ends when the refrigerant reaches a critical vapor quality x_{crit}. The full boiling zone, in turn, is divided into two regions, the first region occurring at the beginning of the boiling process of the refrigerant, where the mixture is rich in liquid, with nucleated boiling as the predominant heat transfer mechanism. As the fluid drains, the quality and velocity of the vapor phase increase, culminating in the second region, which has forced convection as the predominant heat transfer mechanism. Convection heat transfer progressively increases with the flow of the refrigerant to the point where the nucleated boiling disappears. There is a position in the tube where the liquid no longer wets the wall, giving rise to the second part of the boiling process, called a deficient liquid zone, starting with the critical quality and developing until the refrigerant reaches the saturated vapor state. Collier and Thome (1996) present the correlation of Chen (1966), according to Eq. (19), for the calculation of the heat transfer coefficient of the region of full boiling of the refrigerant $H_{f_{b_{full}}}$ for a specific vapor quality.

$$H_{f_{b_{full}}} = F_{chen}\, H_{conv_{dittus}} + S_{chen}\, H_{b_{\text{forster}}} \tag{19}$$

Where $H_{conv_{dittus}}$ and $H_{b_{\text{forster}}}$ represent, respectively, the contribution of forced convection and nucleated boiling, and F_{chen} and S_{chen} represent, respectively, the increase factor of the convective effect and the suppression factor of the

nucleated boiling. The $H_{conv_{dittus}}$ is determined by the correlation of Dittus and Boelter (1930) for the case of heating, given by Eq. (20).

$$Nu_{f_l} = 0{,}023 Re_{f_l}^{0,8} Pr_{f_l}^{0,4} \tag{20}$$

Where Nu_{f_l} is the Nusselt number of the saturated liquid given by Eq. (21), valid for Reynolds number of the fluid in the saturated liquid state Re_{f_l} higher then 2300. For the case of $Re_{f_l} \leq 2300$, Eq. (22), suggested by Incropera et al. (2007) for the situation where the wall temperature is constant can be used.

$$Nu_{f_l} = \frac{H_{conv_{dittus}} d_{in_f}}{k_{f_l}} \tag{21}$$

$$Nu_{f_l} = 3{,}66 \tag{22}$$

Where Pr_{f_l} is the Prandtl number and k_{f_l} is the thermal conductivity of the refrigerant in the saturated liquid state. Re_{f_l} is given by Eq. (23). The thermophysical properties of the refrigerant relative to the saturated liquid state are related to the boiling temperature. The factor F_{chen} is given by Eq. (24) and χ is the parameter of Lockhart and Martinelli (1949), given by Eq. (25).

$$Re_{f_l} = \frac{G_f (1-x) d_{in_f}}{\mu_{f_l}} \tag{23}$$

$$\begin{cases} F_{chen} = 1, \ para \ \frac{1}{\chi} < 0{,}1 \\ F_{chen} = 2{,}35 \left(\frac{1}{\chi} + 0{,}213\right)^{0,736}, \ para \ \frac{1}{\chi} \geq 0{,}1 \end{cases} \tag{24}$$

$$\chi = \left(\frac{1-x}{x}\right)^{0,9} \left(\frac{\rho_{f_l}}{\rho_{f_v}}\right)^{0,5} \left(\frac{\mu_{f_l}}{\mu_{f_v}}\right)^{0,1} \tag{25}$$

Where ρ_{f_l} and ρ_{f_v} are, respectively, the specific masses of the refrigerant in the saturated liquid and saturated vapor states. In addition, μ_{f_v} is the dynamic viscosity of the refrigerant in the saturated vapor state. The thermophysical properties of the refrigerant in the saturated vapor state are correlated to the boiling temperature. The $H_{b_{\text{forster}}}$ is determined by the correlation of Forster and Zuber (1955), given by Eq. (26).

$$H_{b_{\text{forster}}} = 0{,}00122 \frac{{k_{f_l}}^{0,79} {cp_{f_l}}^{0,45} {\rho_{f_l}}^{0,49}}{\sigma^{0,5} {\mu_{f_l}}^{0,29} {h_{lv_f}}^{0,24} {\rho_{f_v}}^{0,24}} \Delta T_{sat}^{0,24} \Delta P_{sat}^{0,75} \tag{26}$$

Where cp_{f_l} is the specific heat of the refrigerant in the saturated liquid state. σ is the surface tension of the refrigerant. h_{lv_f} is the refrigerant vaporization latent specific heat. ΔT_{sat} is the difference between the temperature of the wall in the region and the refrigerant saturation temperature (temperature of boiling point) and ΔP_{sat} is the pressure difference between the saturated vapor of the refrigerant at the wall temperature and the saturated vapor of the refrigerant at the saturation temperature. The factor S_{chen} is given by Eq. (27).

$$S_{chen} = \frac{1}{1 + 2{,}53x10^{-6} {Re_{f_b}}^{1,12}} \tag{27}$$

On what Re_{f_b} is the Reynolds number of the refrigerant in the biphasic state, given by Eq. (28). Chen's correlation (1966) is valid for $1{,}4x10^4 \leq Re_{f_b} \leq 3{,}4x10^5$ and $0{,}001 \leq \chi \leq 1$. x_{crit} can be calculated by the correlation of Sthapak, Varma and Gupta (1975), given by Eq. (29).

$$Re_{f_b} = Re_{f_l} F_{chen}^{1,25} \tag{28}$$

$$x_{crit} = 7{,}943 \left[Re_{f_v} \left(2{,}03x10^4 Re_{f_v}^{-0,8} \Delta T_{sat} - 1\right)\right]^{-0,161} \tag{29}$$

Where Re_{f_v} is the Reynolds number of the refrigerant in the saturated steam state, given by Eq. (30). However, as the vapor quality of the refrigerant fluid varies throughout the process, Chen's correlation (1966) is applied to the quality starting from x_{in} until x_{crit} in order to consider its linear variation.

$$Re_{f_v} = \frac{G_f x d_{in_f}}{\mu_{f_v}} \tag{30}$$

For the liquid-deficient region, the Chen (1966) correlation is not applicable. For this region there are other appropriate correlations. However, when applied, there would be a discontinuity in the heat transfer coefficient at the critical quality point and a discontinuity at the quality point corresponding to the saturated vapor. As a result, Wang and Touber (1991) proposed a second degree polynomial, given by Eq. (31), to estimate the heat transfer coefficient in the liquid deficient zone $H_{f_{b_{def}}}$, ensuring the continuity of this coefficient between the three regions of the heating process (full boiling zone, deficient liquid zone and steam overheating zone).

$$H_{f_{b_{def}}} = a_0 + a_1 x + a_2 x^2 \tag{31}$$

Where a_0, a_1 and a_2 are polynomial constants calculated from three conditions to maintain the continuity of the heat transfer coefficient in the liquid deficient zone. The first condition is that at the entrance of this zone the coefficient is the same as that calculated at the exit of the zone of full boiling (with a critical quality). The second is that at the exit of the liquid deficient zone, the coefficient is the same as that calculated for the beginning of the superheat region (with the saturated steam quality). Finally, the third condition is that at the entrance of the liquid deficient zone, the derivative of Eq. (31) in relation to x be zero, avoiding an abrupt transition at the border point between the full boiling zone and the liquid deficient zone.

Finally, the total boiling region is divided into 200 parts and the value of H_{f_b} used in the project is given by Eq. (32), being j the j-th variable or parameter analyzed, which in this case corresponds to the boundary with x_{crit} .

$$H_{f_b} = \frac{\sum_{i=1}^{j} H_{f_{b_{full_i}}} + \sum_{i=j}^{N} H_{f_{b_{def_i}}}}{N} \tag{32}$$

The H_{amb} represents the contribution of all energy provided by the environment, given by Eq. (33). In which H_{air}, H_{rad} and H_{solar} are, respectively, the coefficients of heat transfer through air, by ambient radiation and by solar irradiation.

$$H_{amb} = H_{air} + H_{rad} + H_{solar} \tag{33}$$

The heat transfer coefficient by air is dependent on three parts: natural convection $H_{air_{nat}}$, forced convection $H_{air_{conv}}$ (the first two being classified as sensitive heat) and condensation of water vapor present in the air $H_{air_{co}}$ (the latter being classified as latent heat). The natural convective coefficient of heat transmission through the air is given by Eq. (34).

$$H_{air_{nat}} = \frac{Nu_{air_{nat}} k_{air}}{L_{pl}} \tag{34}$$

Where k_{air} is the air thermal conductivity coefficient and $Nu_{air_{nat}}$ is the Nusselt number for natural convection. To determine $H_{air_{nat}}$, Incropera et al. (2007) recommend the correlation of Churchill and Chu (1975), given by Eq. (35).

$$Nu_{air_{nat}} = \left\{ 0{,}825 + \frac{0{,}387 {Ra_{air}}^{1/6}}{\left[1+(0{,}492/Pr_{air})^{9/16}\right]^{8/27}} \right\}^2 \tag{35}$$

Where Pr_{air} is the air Prandtl number and Ra_{air} is the air Rayleigh number given by Eq. (36), adapted for the case of an inclined flat plate. It is to remarc that for the application of the correlation of Churchill and Chu (1975), all the thermophysical properties of the fluid must be obtained at the film temperature (average between the temperature of the wall and that of the air).

$$Ra_{air} = \frac{g cos\theta \beta_{air} (T_{air} - T_w) L_{pl}^3}{\alpha_{air} \upsilon_{air}} \tag{36}$$

Where β_{air} is the air thermal volumetric expansion coefficient, T_w it is the temperature of the evaporator tube wall (weighted average of the wall temperatures of the boiling and overheating regions, considering the respective lengths of

these regions), α_{air} is the thermal diffusivity of the air and υ_{air} is the air kinematic viscosity. The forced convective coefficient of heat transmission through the air is given by Eq. (37).

$$H_{air_{for}} = \frac{Nu_{air_{for}} k_{air}}{L_{pl}} \tag{37}$$

Where $Nu_{air_{for}}$ is the Nusselt number for the forced convection performed by the action of the wind. Incropera et al. (2007) recommend Eq. (38) (turbulent regime) and Eq. (39) (laminar regime) for the case of a flat plate with constant thermal flow. It is worth mentioning that, since the contribution via forced convection heat occurs only in the outdoor condition, its effect considered in the dimensioning of the evaporator is only 50% of the estimated.

$$Nu_{air_{for}} = 0{,}0308 Re_{air}^{4/5} Pr_{air}^{1/3} \tag{38}$$

$$Nu_{air_{for}} = 0{,}453 Re_{air}^{1/2} Pr_{air}^{1/3} \tag{39}$$

The expressions are valid for $0{,}6 \leq Pr_{air} \leq 60$ turbulent and $Pr_{air} < 0{,}6$ laminar regimes. Where Re_{air} is the air Reynolds number, given by Eq. (40).

$$Re_{air} = \frac{V_{air} L_{pl}}{\upsilon_{air}} \tag{40}$$

The evaporator is simultaneously affected by the two forms of sensitive heat transfer mentioned above (mixed convection). To assess the relevance of each of them in the phenomenon it is necessary to determine the value of the ratio Gr_{air}/Re_{air}^2, where Gr_{air} is the number of Grashof, being obtained through Eq. (41).

$$Ra_{air} = Gr_{air} Pr_{air} \tag{41}$$

Incropera et al. (2007) recommend Eq. (42) for the case of a flat plate that suffers an air cross flow in relation to the flow of the refrigerant (perpendicular directions) in order to determine the Nusselt number of the air related to the transmission of sensitive heat $Nu_{air_{sen}}$ when $Gr_{air}/Re_{air}^2 \approx 1$. In the case $Gr_{air}/Re_{air}^2 \ll 1$, natural convection is neglected, and for $Gr_{air}/Re_{air}^2 \gg 1$ forced convection is neglected. The air sensitive heat transmission coefficient $H_{ar_{sen}}$ is then given by an equation analogous to Eq. (37).

$$Nu_{air_{sen}}^3 = Nu_{air_{nat}}^3 + Nu_{air_{for}}^3 \tag{42}$$

Due to the relative humidity of the air, the water vapor present in the air can undergo condensation on the cold surface of the evaporator if it is at a temperature equal to or below the temperature corresponding to the dew point. For the determination of the heat transfer coefficient by condensation, the methodology proposed by Scarpa and Tagliafico (2016), who used Eq. (43) and Eq. (44) was used. These equations take into account the dilution of water vapor in atmospheric air. This approach consists of calculating the mass transfer coefficient H_m for the condensation of a very diluted system on a cold surface (similar to the heat and mass transfer) from the knowledge of the $H_{air_{sen}}$ in the air and evaporator interface.

$$H_m = \frac{H_{air_{sen}}}{c_{p_{air}} \rho_{air} R_{wv} T_{air}} \left(\frac{P_{atm}}{P_{part(T_{air})} - P_{sat(T_w)}} \right) In \left[\frac{P_{atm} - P_{sat(T_w)}}{P_{atm} - P_{part(T_{air})}} \right] \tag{43}$$

$$\dot{Q}_{air_{co}} = H_m (2\eta_{fin} A_{fin} + A_b)(P_{air_v} - P_{air_{sat_w}}) h_{lv_{wv}} \tag{44}$$

Where $c_{p_{air}}$ is the specific heat at constant pressure for the air. ρ_{air} is the specific mass of the air. T_{air} is given in Kelvin. $R_{wv} = 461{,}5\ J/kg.K$ is the gas constant of the water vapor. $P_{part(T_{air})}$ is the partial pressure of vapor in the air measured in the air temperature and given by Eq (45). $P_{sat(T_w)}$ is the saturation pressure of the vapor measured at the wall temperature T_w. $h_{lv_{wv}}$ is the specific latent heat of water vaporization measured at the dew temperature T_d and $\dot{Q}_{air_{co}}$ is the rate of heat by condensation of the water vapor transferred to the evaporator and given by Eq. (46). The two faces of the fin are exposed to heat exchange by latent heat.

$$P_{part(T_{air})} = \phi P_{sat(T_{air})} \tag{45}$$

$$\dot{Q}_{air_{co}} = H_{air_{co}}(2\eta_{fin}A_{fin} + A_b)(T_d - T_w) \tag{46}$$

Where $P_{sat(T_{air})}$ is the vapor saturation pressure measured at air temperature. The wall temperature is obtained by the weighted average of the boiling and overheating regions, taking into account the respective lengths. The length and wall temperature of the superheat region are shown later. It is worth noting that, as the contribution by latent heat occurs only in the indoor condition, its effect considered in the design of the evaporator is only 50% of the estimated. Finally, H_{air} is given by Eq. (47).

$$H_{air} = H_{air_{sen}} + H_{air_{co}} \tag{47}$$

The coefficient of heat transfer by ambient radiation is given by Eq. (48). Where σ_{SB} is the constant of Stefan-Boltzmann (5,67 x 10^{-8} W/m^2. K^4). The temperatures in Eq. (48) are given in Kelvin.

$$H_{rad} = \varepsilon\sigma_{SB}(T_{sur} + T_w)(T_{sur}^2 + T_w^2) \tag{48}$$

The heat transfer coefficient by solar irradiation is obtained by means of Eq. (49) and Eq. (50). Where $\dot{Q}_{solar}$ is the rate of heat exchanged for solar radiation. Only one face of the fin is exposed to this type of heat exchange.

$$\dot{Q}_{solar} = \alpha I_{solar}\left(\eta_{fin}A_{fin} + \frac{A_b}{2}\right) \tag{49}$$

$$\dot{Q}_{solar} = H_{solar}\left(\eta_{fin}A_{fin} + \frac{A_b}{2}\right)(T_w - T_{sky}) \tag{50}$$

The second region to be dimensioned is that of overheating the refrigerating fluid. This stage is characterized by the increase in the temperature of the refrigerant, corresponding to the degree of overheating, initially in the state of saturated steam at $T_{f_1'}$ (the same as T_{f_b}) until the state of steam overheated in temperature at T_{f_1}. To determine the length of the superheat region L_{SH}, Eq. (51) is used.

$$\dot{Q}_{SH} = U_{SH}\pi d_{out_f}L_{SH}\left(T_{amb} - \frac{T_{f_1'} + T_{f_1}}{2}\right) \tag{51}$$

Where U_{SH} is the global coefficient of the refrigerant fluid in the superheat region given by Eq. (52) and the wall temperature $T_{w_{SH}}$ in the region is given by Eq. (53).

$$\frac{1}{U_{SH}} = \frac{1}{H_{amb}} + \frac{d_{out_f}}{H_{f_{SH}}d_{in_f}} + \frac{d_{out_f}ln\left(\frac{d_{out_f}}{d_{in_f}}\right)}{2k_w} \tag{52}$$

$$T_{w_{SH}} = \frac{H_{f_{SH}}\frac{T_{f_1'} + T_{f_1}}{2} + H_{amb}T_{amb}}{H_{f_{SH}} + H_{amb}} \tag{53}$$

Where $H_{f_{SH}}$ is the refrigeranting fluid internal heat transfer coefficient in the superheat region, being determined through the correlation of Dittus and Boelter (1930) for the case of heating, as presented by Eq. (54) and Eq. (55).

$$Nu_{f_v} = 0{,}023Re_{f_v}^{0,8}Pr_{f_v}^{0,4} \tag{54}$$

$$Nu_{f_v} = \frac{H_{f_{SH}}d_{in_f}}{k_{f_v}} \tag{55}$$

On what Pr_{f_v} is the Prandtl number and k_{f_v} is the thermal conductivity of the refrigerant in the saturated vapor state. The total length of the evaporator is the sum of the lengths obtained for the two regions, given by Eq. (56).

$$L_{evap} = L_b + L_{SH} \tag{56}$$

Given the modeling that allows the design of the evaporator, it is possible to determine the other heat rates exchanged with the component, making it possible to estimate the efficiency of the evaporator. The rate of heat exchanged for air via sensitive heat $\dot{Q}_{air_{sen}}$ is given by Eq. (57). The two faces of the fin are exposed to ambient radiation.

$$\dot{Q}_{air_{sen}} = H_{air_{sen}}\left(2\eta_{fin}A_{fin} + A_b\right)\left(T_{air} - T_w\right) \tag{57}$$

The rate of heat exchanged due to ambient radiation $\dot{Q}_{rad}$ is given by Eq. (58). The two faces of the fin are exposed to ambient radiation. Finally, the efficiency of the solar evaporator η_{evap} can be given by Eq. (59). Where $\dot{Q}_{evap_{av}}$ is the rate of total heat available for the evaporator by the environment, and is given by Eq. (60).

$$\dot{Q}_{rad} = H_{rad}(2\eta_{fin}A_{fin} + A_b)\left(T_{sur} - T_w\right) \tag{58}$$

$$\eta_{evap} = \frac{\dot{Q}_{evap}}{\dot{Q}_{evap_{av}}} \tag{59}$$

$$\dot{Q}_{evap_{av}} = \dot{Q}_{air_{sen}} + \dot{Q}_{air_{co}} + \dot{Q}_{rad} + \dot{Q}_{solar} \tag{60}$$

The evaporator efficiency represents the proportion of heat from the environment that is received by the evaporator and is used by the refrigerant in its expansion. In addition, it indicates how well dimensioned the component is for the system operating under certain environmental conditions. This parameter is important for optimizing the size of the heat exchanger, which can result in material savings for its manufacture.

2.3 Determination of refrigerant mass

The mass of refrigerant in the heat exchangers and in the equipment as a whole is an impacting factor in determining the TEWI of the system. The calculation of the total mass of fluid in the heat exchangers is divided into two regions: single-phase and two-phase. The single-phase region appears in the evaporator only in the overheating section. The Eq. (61) allows the determination of the m_{mon} mass in the single-phase regions of the system.

$$m_{mon} = \sum_{i=1}^{N} \rho_{mon_i} \forall_i \tag{61}$$

Where ρ_{mon_i} and $\forall_i$ are, respectively, the specific mass in the single-phase region and the volume occupied by the refrigerant in each division of the tube. The index *i* represents the *i-th* variable. The biphasic region appears in the evaporator at the boiling section. The Eq.(62) allows the determination of the mass m_{bip} in the biphasic regions of the system. It is considered N= 200 divisions for all biphasic regions of the system.

$$m_{bip} = \sum_{i=1}^{N} [\alpha_{void_i}\rho_v + \left(1 - \alpha_{void_i}\right)\rho_l]\forall_i \tag{62}$$

Where ρ_l and ρ_v are, respectively, the specific masses of the refrigerant in the liquid saturated state and saturated steam. The term α_{void_i} represents the void fraction of the refrigerant in each division of the pipe and can be determined by the Rouhani and Axelsson (1970) modified Steiner (1993) correlation given by Eq.(63) and Eq.(64), where C_o is a parameter of the correlation.

$$\alpha_{void} = \frac{x}{\rho_v}\left[C_o\left(\frac{x}{\rho_v} + \frac{1-x}{\rho_l}\right) + \left(\frac{1{,}18(1-x)[g\sigma(\rho_l - \rho_v)]^{0,25}}{G_f \rho_l^{0,5}}\right)\right]^{-1} \tag{63}$$

$$C_o = 1 + 0{,}12(1-x) \tag{64}$$

Where σ is the refrigerant surface tension and g is the gravity acceleration. The sizing of the heat exchangers makes it possible to determine the required mass when it operates with a given refrigerant. The average of the masses required by the two condensers was considered in order to simplify the simulations. The solar evaporator was also dimensioned and the mass of refrigerant required was also calculated.

3. RESULTS

Table 4 shows the total mass in the heat exchangers and the result of the TEWI and COP. The refrigerants are arranged in ascending order of TEWI.

Table 4. TEWI for Heat Exchangers.

Fluid	T crit. (ºC)	P crit. (kPa)	GWP	Mass Heat exchan. (kg)	COP	TEWI direct	TEWI indirect	TEWI
R744	31	7377	1	0.2636	2.90	0.57	1532	1532

Fluid	T crit. (ºC)	P crit. (kPa)	GWP	Mass Heat exchan. (kg)	COP	TEWI direct	TEWI indirect	TEWI
R152a	113.3	4517	140	0.1186	2.80	36.12	1582	1618
R1233zd(E)	165.6	3580	1	0.1230	2.18	0.27	2038	2038
R290	96.7	4251	5	0.0758	2.12	0.82	2089	2090
R600	152	3796	4	0.0583	1.98	0.51	2242	2243
R1234ze(E)	109.4	3632	1	0.1467	1.88	0.32	2361	2362
R600a	134.7	3629	20	0.0632	1.88	2.75	2365	2368
R170	32.7	4872	5.5	0.1084	1.85	1.30	2397	2398
R134a	101	4059	1300	0.1625	2.21	459.53	2008	2467
R1234yf	94.7	3382	1	0.1447	1.70	0.31	2607	2607

Regarding the environmental performance of the refrigerants applied in the heat exchangers, the R744 presents itself as the best option, besides providing the best energy efficiency. Then there is R152a, also responsible for the second best COP. In third place comes R1233zd(E), in fourth place comes R290 and in fifth place comes R600. Adopting R134a as the refrigerant to be replaced, R744 presents TEWI 38% better, while R152a, R1233zd(E), R290 and R600 present environmental performance, respectively, 34, 17, 15 and 9% better when applied in heat exchangers.

For refrigerants with very low GWP, the mass has a negligible influence, since it only influences the direct TEWI, and this value is close to 1. The indirect TEWI is preponderantly high in relation to the direct TEWI and depends directly on the COP, being very sensitive to the influence of this parameter. This explains why R744 is the best option, since it provides the best COP even with the largest mass request.

Considering the results of the simulations and from an environmental performance point of view, the R744 is the best choice to operate in a small Heat Pump (heating power around 1 kW). However, from a logistical point of view, no compressor is for sale in the country that operates with this fluid. The same happens with R152a and R1233zd(E). As the design premise is a low cost heat pump and the import of components from other countries makes the manufacture of the system significantly more expensive, these fluids are not considered. Thus, R290 is chosen, having low cost and wide availability in the national market, both in terms of the refrigerant itself, and in terms of compressor and auxiliary components.

3.1 Results of the solar evaporator project

The length of the solar evaporator required to operate the R290 is 15.3 m. By simulation, the mass of refrigerant required by the evaporator to operate with the R290 is approximately 35 g. The solar evaporator was manufactured and is available to be inserted in the system. In the manufacturing process, a plate with final dimensions 1.03 m wide and 1.60 m long was formed in the serpentine tube, resulting in 10 fins segments. The distance between the tubes center to center is 103 mm and the characteristic length of the fin is 46.74 mm. Figure 2 shows the design of the tube in serpentine shape and Figure 3 shows the solar evaporator after its manufacture. The evaporator received a layer of matte black paint over its entire surface to optimize the absorption of heat by irradiation.

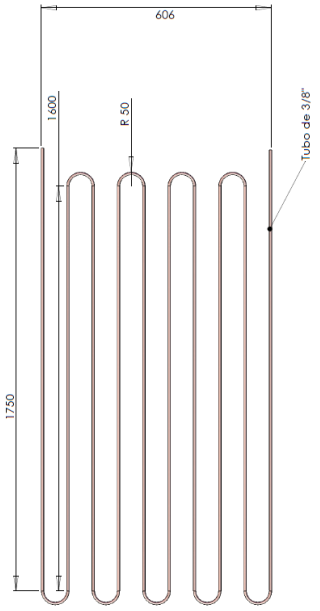

Figure 2: Solar evaporator design

Figure 3: Manufactured solar evaporator.

4. CONCLUSIONS

The application of a DX-SAHP in water heating proves to be an optimal sustainable solution and the best alternative among heat pumps for this purpose. The sizing of the heat exchangers and the determination of the mass required by them and the rest of the system enables the analysis of the environmental and logistic performance (relative to the construction of the system) of 10 selected refrigerants (R134a, R152a, R744, R1234yf, R1234ze(E), R1233zd(E), R170, R290, R600 and R600a). As a result, R290 is selected to operate the proposed system.

The dimensioned solar evaporator has a length of 16.0 m. The refrigerant mass required by this exchanger is 35 g.

This work allowed the development of a useful tool to size the evaporator, making it possible to select the appropriate ecological refrigerant from a solar heat pump for the required operating conditions. Furthermore, the application of this tool provides the analysis of the thermal and environmental performance of a DX-SAHP and its retrofit, simulating the application of different refrigerants.

5. ACKNOWLEDGEMENTS

This work was supported by the Foundation for Research Support of the State of Minas Gerais (FAPEMIG), National Council for Scientific and Technological Development (CNPq) and Coordination of Improvement of Higher Level Personnel (CAPES).

6. REFERENCES

AIRAH - The Australian Institute of Refrigeration, Air Conditioning and Heating, 2012. Methods of calculating total equivalent warming impact (TEWI) 2012. Fitzroy.

Antunes, AHP and Bandarra Filho, EP, 2016. “Experimental investigation on the performance and global environmental impact of a refrigeration system retrofitted with alternative refrigerants”. International Journal of Refrigeration, vol. 70, p. 119-127.

ASHRAE - American Society of Heating, Refrigerating and Air-Conditioning Engineers, 2017. Handbook - Fundamentals (SI Edition). Atlanta.

Bai, C .; Han, Z., Wei, H., Ju, X., Meng, X. and Fu, Q .. 2020. “Simulation study on performance of a dual-source hybrid heat pump unit with alternative refrigerants”. Energy and Built Environment, vol. 1, p. 1-10.

Barve, A. and Cremaschi, L., 2012. “Drop-in performance of low-GWP refrigerants in a heat pump system for residential application”. International Refrigeration and Air Conditioning Conference at Purdue University, West Lafayette.

Bobbo, S .; Zilio, C .; Scattolini, M .; Fedele, L., 2014. “R1234yf as a substitute of R134a in automotive air conditioning. Solubility measurements in two commercial PAG oils ”. International Journal of Refrigeration, vol. 40, p. 302-308.

Chen, J. C., 1966. “Correlation for Boiling Heat Transfer to Saturated Fluids in Convective Flow”. Industrial & Engineering Chemistry Process Design and Development, vol. 5, p. 322-329.

Churchill, S. W. and Chu, H. H. S., 1975. “Correlating equations for laminar and turbulent free convection from a vertical plate”. International Journal of Heat and Mass Transfer, vol. 18, p. 1323-1329.

Collier, J. G. and Thome, J. R., 1996. Convective boiling and condensation, 3th edition, Oxford University Press Inc., New York.

Diniz, H.A.G., 2017. *Estudo comparativo da eficiência energética de uma bomba de calor assistida por energia solar operando com condensadores por imersão e coaxial*. Master’s thesis, Post-Graduate Program in Mechanical Engineering, Federal University of Minas Gerais, Belo Horizonte.

Dittus, F. W., and Boelter, L. M. K., 1930. “Heat transfer in automobile radiators of the tubular type”. University of California Publication on Engineering, vol. 2, No. 13, Berkeley.

Duarte, WM., 2018. Numeric model of a direct expansion solar assisted heat pump water heater operating with low GWP refrigerants (R1234yf, R290, R600a and R744) for replacement of R134a. Ph.D. thesis, Post-Graduate Program in Mechanical Engineering, Federal University of Minas Gerais (UFMG), Belo Horizonte, Brazil.

Duarte, WM; Paulino, TF; Pabon, JJG; Sawalha, S. and Machado, L., 2019. “Refrigerants selection for a direct expansion solar assisted heat pump for domestic hot water”. Solar Energy, vol. 184, p. 527-538.

Faria, R.N., 2013. *Projeto e construção de uma bomba de calor a CO_2 operando em ciclo transcrítico e modelagem dinâmica do conjunto evaporador solar-válvula de expansão*. Ph.D. thesis, Post-Graduate Program in Mechanical Engineering, Federal University of Minas Gerais, Belo Horizonte.

Forster, H. K. and Zuber, N., 1955. "Dynamics of vapor bubbles and boiling heat transfer". Chemical Engineering Progress, vol. 1, p. 531-535.

Incropera, F. P.; Dewitt, D. P.; Bergman, T. L. and Lavine, A. S., 2007. Fundamentals of Heat and Mass Transfer. 6th edition, Hoboken: John Wiley and Sons.

Ju, F .; Fan, X .; Chen, Y .; Ouyang, H .; Kuang, A .; Ma, S. and Wang, F., 2018a. "Experiment and simulation study on performances of heat pump water heater using blend of R744 / R290". Energy & Buildings, vol. 169, p. 148-156.

Ju, F .; Fan, X .; Chen, Y .; Wang, T .; Tang, X .; Kuang, A .; Ma, S., 2018b. "Experimental investigation on a heat pump water heater using R744 / R290 mixture for domestic hot water". International Journal of Thermal Sciences, vol. 132, p. 1-13.

Ju, F .; Fan, X .; Chen, Y .; Zhang, H .; Wang, T. and Tang, X., 2017. "Performance assessment of heat pump water heaters with R1233zd (E) / HCs binary mixtures". Applied Thermal Engineering, vol. 123, p. 1345–1355.

Klein, SA and Alranrado, FL, 2015. Engineering Equation Solver, EES, Version 10. F-Chart Software, www.fchart.com. Wisconsin Madison.

Koyama, S .; Miyazaki, T .; Hirayama, J .; Takata, N. and Higashi, Y., 2018. "Performance Evaluation of Heat Pump Cycle using Low GWP Refrigerant Mixtures of HFC-32 and HFO-1123". International Refrigeration and Air Conditioning Conference at Purdue University, West Lafayette.

Koury, R. N. N., 1998. Modelagem numérica de uma máquina frigorífica de compressão de vapor. Ph.D. thesis. Post-Graduate Program in Mechanical Engineering, State University of São Paulo, Campinas, Brazil.

Lockhart, R. W. and Martinelli, R. C., 1949. "Proposed correlations of data for isothermal two-phase, two-component flow in a pipe". Chemical Engineering Progress, vol. 45, p. 39-48.

Makhnatch, P. and Khodabandeh, R., 2014a. "Selection of low GWP refrigerant for heat pump by assessing the life cycle climate performance (LCCP)". 11th IEA Heat Pump Conference. Montréal.

Makhnatch, P. and Khodabandeh, R .., 2014b. "The role of environmental metrics (GWP, TEWI, LCCP) in the selection of low GWP refrigerant". Energy Procedia, vol. 61, p. 2460-2463.

Nawaz, K .; Shen, B .; Elatar, A .; Baxter, V. and Abdelaziz, O., 2017a. "R1234yf and R1234ze (E) the low-GWP refrigerants for residential heat pump water heaters". International Journal of Refrigeration, vol. 82, p. 348-365.

Nawaz, K .; Shen, B .; Elatar, A .; Baxter, V. and Abdelaziz, O., 2017b. "R290 (propane) and R600a (isobutane) as natural refrigerants for residential heat pump water heaters". Applied Thermal Engineering, vol. 127, p. 870-883.

Oliveira, R. N., 2013. *Modelo dinâmico e estudo experimental para um resfriador de uma bomba de calor operando com CO_2 para aquecimento de água residencial*. Ph.D. thesis, Post-Graduate Program in Mechanical Engineering, Federal University of Minas Gerais (UFMG), Belo Horizonte, Brazil.

Park, KJ and Jung, D., 2009. "Performance of heat pumps charged with R170 / R290 mixture". Applied Energy, vol. 86, p. 2598-2603.

Paula, CH; Duarte, WM; Rocha, TTM; Oliveira, RNO and Maia, AAT, 2019. "Environmental and energy performance evaluation of the R1234yf as an environmentally friendly alternative to R134a". 25th International Congress of Mechanical Engineering - COBEM. Uberlândia.

Reis, R.V.M, 2012. *Análise experimental comparativa entre uma bomba de calor e uma resistência elétrica como dispositivo de apoio de energia para um aquecedor solar de água*. Ph.D. thesis, Post-Graduate Program in Mechanical Engineering, Federal University of Minas Gerais, Belo Horizonte.

Rodríguez, O.R.S., 2015. *Desenvolvimento de um simulador de coletor solar para reprodução das condições de operação de uma bomba de calor para aquecimento de água residencial*. Master's thesis, Post-Graduate Program in Mechanical Engineering, Federal University of Minas Gerais, Belo Horizonte.

Ruas, S.N.R., 2018. *Estudo experimental sobre o desempenho de uma bomba de calor a CO_2 assistida por energia solar de expansão direta para aquecimento de água para uso residencial*. Ph.D. thesis, Post-Graduate Program in Mechanical Engineering, Federal University of Minas Gerais, Belo Horizonte.

Scarpa, F. and Tagliafico, L. A., 2016. "Exploitation of humid air latent heat by means of solar assisted heat pumps operating below the dew point". Applied Thermal Engineering, vol. 100, p. 820-828.

Sthapak, H.; Varma, H. K. and Gupta, C. P., 1975. Mass vapour fraction at the onset of dryout in a horizontal tube evaporator, XII International Congress of Refrigeration, p. 318-324, Moscou.

UNEP - United Nations Environment Program, 2016. The Montreal Protocol on Substances that Deplete the Ozone Layer. Kigali.

Wang, H. and Touber, S., 1991. "Distributed and non-steady-state modelling of an air cooler". International Journal of Refrigeration, vol. 14, p. 98-111.

Xiao, B .; Chang, H .; He, L .; Zhao, S. and Shu, S., 2020. "Annual performance analysis of an air source heat pump water heater using a new eco-friendly refrigerant mixture as an alternative to R134a". Renewable Energy, vol. 147, p. 2013-2023.

Zhang, M. and Muehlbauer, J., 2012. "Life cycle climate performance model for residential heat pump systems". International Refrigeration and Air Conditioning Conference at Purdue University, West Lafayette.

7. RESPONSIBILITY NOTICE

The authors are the only responsible for the printed material included in this paper.